H1-02/96-471
February 10, 1996

An Offline Luminosity Determination for the 1995 H1 e^+p Data

N. Gogitidze[1] and S. Levonian[1,2]

[1] Lebedev Physical Institute, Moscow, Russia
[2] LPNHE, Ecole Polytechnique, Palaiseau, France

Abstract

A procedure is described to calculate an integrated luminosity using the photon energy spectrum from $ep \to e\gamma p$ bremsstrahlung events. It is applied to the 1995 data accumulated by the H1 experiment. Major corrections to the online measurements are related to the electron tagger acceptance variations with the changing beam conditions and to the proton satellite bunch effect. The precision of the integrated luminosity is determined for three data samples: the one with the nominal position of the Interaction Point, and those with the IP shifted by ± 70 cm along the z axis.

1 Introduction

So far the best method of the luminosity measurement at HERA, used by both the H1 and the ZEUS experiments, is the one based on Bethe-Heitler reaction (hereafter referenced as BH)

$$ep \to e\gamma p. \tag{1}$$

The instantaneous (L) and integrated ($\mathcal{L}$) luminosities are then calculated as

$$L = \frac{R_{BH}}{\sigma_{BH}}; \qquad \mathcal{L} = \frac{N_{BH}}{\sigma_{BH}}, \tag{2}$$

where R, N, σ denote the rate, the number of events and the cross section [1] of the reaction (1) correspondingly. There are however several technically different methods to identify the reaction (1) and to calculate R (or N) in (2):

- a *coincidence* method (used online by the H1 Luminosity Monitor) requires to detect both e and γ simultaneously in the final state,
- a *single photon* method (used by the ZEUS Luminosity Monitor) counts the rate (the number of events) in (2) with the photon energy above a certain threshold,
- an *energy flow* method (so far not exploited at HERA) which measures a total γ energy flux (instead of the event rate), thus partly accounting for the pile-up effect at high beam intensities, etc.

The discussion on the advantages and drawbacks of these methods can be found in [2, 3]. Offline, we use a *single photon method* for the final value of the integrated luminosity $\mathcal{L}$ determined from reaction (1).

Equations (2) look quite simple. Complications come when trying to relate a number of observed events to the true value, predicted by theory, and to calculate the acceptance corrected cross section σ_{BH}. Then in practice an integrated luminosity for the given data sample can be determined as

$$\mathcal{L} = \frac{N^{ep}_{BH}(E_\gamma > E_{min})}{\sigma_{BH}(E_\gamma > E_{min})} = \frac{\frac{\sum_i (W_i^{tot}(E_{min}) - W_i^{bgr}(E_{min}))}{\epsilon_{trig}(E_{min})}(1 - \delta_{n\gamma}(L, E_{min}))}{\sigma_{BH}(E_{min}) \cdot A_\gamma(\theta_x, \theta_y)}, \tag{3}$$

where $W_i = P_i N_i$ represent the total and the background number of events in run i from the sample, after accounting for the (run dependent) prescaling P_i. In equation (3) for simplicity only the most important parameters are listed in various functional dependencies. The geometrical acceptance A_γ is especially sensitive to the lepton beam tilt θ_x, θ_y in the interaction point (IP). A pile-up effect (the probability to detect more than just one photon in the same bunch crossing) leads to a luminosity dependent correction $\delta_{n\gamma}(L, E_{min})$ in the number of observed events having an energy deposit above the cutoff E_{min}.

A choice of E_{min} represents usually a compromise between several partially conflicting demands, and must be optimized to reduce the final systematic error $\delta\mathcal{L}$.

A general description of the H1 Luminosity System can be found elsewhere [4]. In this note we first describe special luminosity data used for the present analysis. Then, in section 3 all the details are given on the procedure to determine $\mathcal{L}$ according to (3), together with the results obtained. Section 4 is devoted to a preliminary estimate of the satellite bunch corrections. We conclude with the final precision of the luminosity determination in the three basic event samples accumulated by the H1 experiment in 1995.

2 Lumi Data Sample

In order to facilitate the offline monitoring and calibration of the H1 Luminosity system, a special scheme has been set up in 1994 in a framework of the online logging process, creating so called **LUMIMON** data sample. This sample contains in a very compact form all essential Lumi trigger and readout information. As an important practical improvement, a special event classification has been implemented in 1995, allowing fast access to the data, by using the **FPACK** selection mechanism [5]. Some technical details can be found in the Appendix. Further information concerning **LUMIMON** data can be accessed via [6].

A summary of the luminosity monitoring triggers, used in 1995 data taking, is given in table 1. Their total rate amounts to 1.4 Hz. Taking into account an average size of **LUMIMON** event ($\sim$ 3.5 kb) this leads to a comfortable L4 output rate of $\sim$5 kb/s.

Table 1: A list of the luminosity monitoring triggers used in 1995 (see also Appendix for more information on **LUMIMON** sets).

Trigger	Purpose	$<$Prescaling$>$	L1 rate [Hz]
s86	monitoring the background to γp physics	$0.98 \cdot 10^5$	0.14
s90	ET44 monitoring, calibration	$1.50 \cdot 10^5$	0.31
s91	offline $\mathcal{L}$ determination	$4.49 \cdot 10^5$	0.26
s92	calibration of ET and PD	$2.64 \cdot 10^5$	0.09
s93	VC, ET44 calibration, tagging acceptance	$9.05 \cdot 10^5$	0.22
s94	calibration of ET and PD	$0.45 \cdot 10^5$	0.26
s95	Calibration of ET, PD and VC	$4.31 \cdot 10^5$	0.12

A sub-sample of **s91** (**LUMIMON** class 16) was a basis of the present analysis. In addition, randomly triggered events (**LUMIMON** class 9) were used for the trigger efficiency determination. The following filter has been applied to select events for the offline luminosity calculation:

- event belongs to "G" or "M" run (H1EP classification), taken with the H1 magnetic field on (i.e. after July, 7),
- trigger set = 0 (**LUMIMON** class = 26), selecting only ep collision mode (according to the official trigger description!),
- event is triggered by **s91** (`LU_PD_low bit = 1`), i.e. **LUMIMON** class = 16.

Next, the possible sources of event losses have been checked, as well as the presence and the correctness of all necessary information in the database (trigger phase, prescale gaps, etc.).

There were no losses at L4 level found, by analyzing the L4 reject files. Only very few runs taken in L4 transparent mode had to be excluded from the online luminosity table for the correct comparison, because in this case **LUMIMON** classification (which is performed at the filter farm processors) was absent, and hence these runs were not available for the offline analysis.

In order to check the correctness of the prescale gaps for the subtrigger **s91**, we plot in Fig.1 the ratio of the **s91** events to the online $\mathcal{L}$ for each run. Note, that only really large deviations from the general trend are suspicious. The fluctuations within a 20-50% band are acceptable and expected from the changing background conditions and varying trigger threshold (in absolute energy scale). Two runs in this plot: 112850 ($\mathcal{L}$ = 0.014 nb^{-1}) and 118578 ($\mathcal{L}$ = 0.015 nb^{-1}) fall significantly off the overall level and therefore were excluded from the analysis. Their relative contribution is anyway negligibly small.

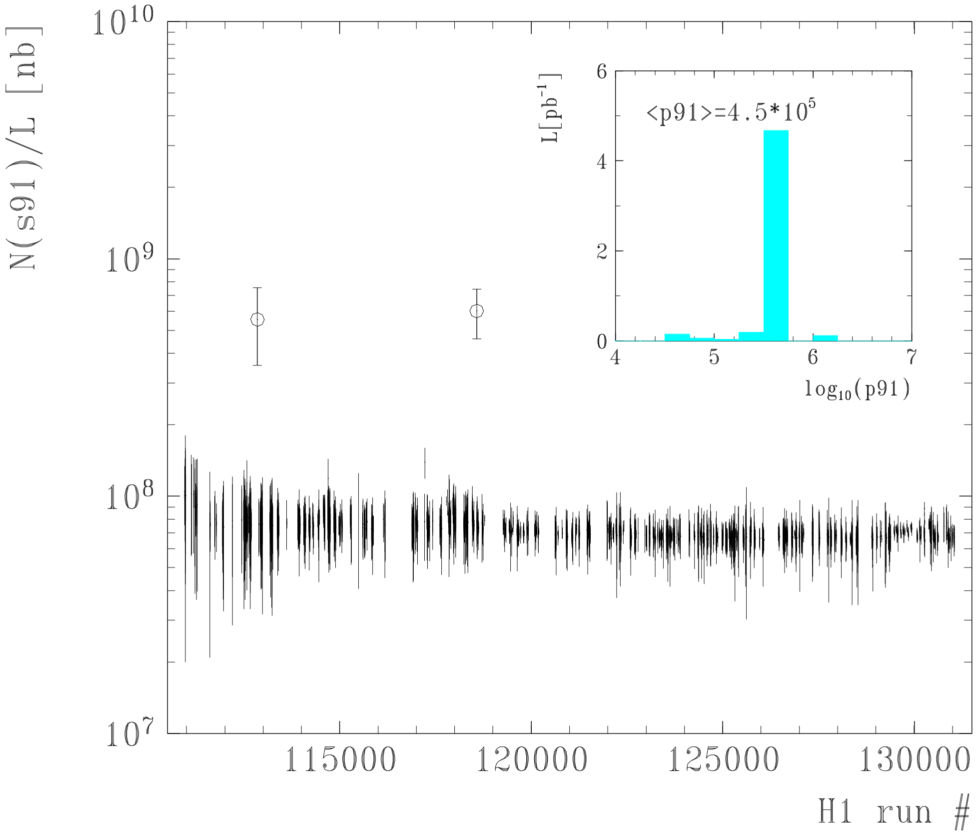

Figure 1: The number of BH events (triggered by **s91**, before L1 prescaling) per nb^{-1} as a function of run number. Two runs (with total $\mathcal{L}$ = 0.03 nb^{-1}) marked by circles, were excluded from the analysis. The insert shows the distribution of the prescale gaps for **s91** trigger in analyzed runs.

The biggest "losses", representing 5.6% of all G and M runs, were caused by the requirement of *trigger set = 0*, which was supposed to contain all the data, taken in *ep* collision mode [7]. It turned out however, that part of the runs (typically in phase 1) were taken with the *trigger set = 3 ("before lumi start up")*, but still were classified as "G" or "M" runs. In order to make the comparison with the online luminosity valid, these runs were also excluded from the online lumi list for the purpose of the present analysis.

Warning: most likely, all these runs (trigger phase 1: no trackers) are anyway not usable for physics, but it must be kept in mind, that they are present in the official list of G and M runs (both in H1EP and in the database). If however they *are* analyzed, the offline luminosity correction from the corresponding run range will be applied to them automatically. There is no reason to assume, that the correction must be different for this small part of runs, compared to the rest of the data.

In total $\boxed{955715}$ events passed the selection and the quality criteria and were used for the offline luminosity determination. A summary of the 1995 luminosity usage is given in table 2.

Table 2: An integrated luminosity in the H1 interaction region, as measured by the online Luminosity Monitor in 1995.

Integrated luminosity	[nb^{-1}]
HERA produced (at final beam energies)	11055
HERA delivered to H1 (lumi declared)	10094
H1 gated (written on tapes)	6196
with magnetic field on (after 7-July-95)	5854
physics (classified as "G" or "M")	5437
used for the present analysis	5132

The data have been split in three different samples according to the position of the Interaction Point along the z axis. Some general characteristics of these data samples are summarized in table 3. For comparison, the parameters of the 1994 nominal IP e^+p sample are also listed there. It is important to stress significantly larger HV corrections for 1995 data, which are in addition analysis dependent. The numbers given in the table are only illustrative, and correspond to the following sub-detectors required to be operational: CJC(1&2), LAr, SPACAL (BEMC for 1994), ToF and LUMI.

Table 3: Characteristics of three different data samples collected by the H1 experiment in 1995. For comparison, the parameters of the 1994 e^+p nominal IP data are also listed. († HV corrections have been evaluated requiring the following sub-detectors to be operational: CJC, LAr, SPACAL(BEMC), ToF, LUMI).

Parameter	Unit	1995			1994
		nominal IP	z_{IP}=+70cm	z_{IP}=−70cm	e^+p
H1 Run range		110896–129387 130403–131045	129462–129934	129974–130385	82961–89928 90101–90419
Number of G+M runs		2890	114	59	1521
<Run time>	[s]	960	976	982	1803
<L1 dead time>	[%]	17.7	10.6	17.1	13.0
Online $\mathcal{L}$	[nb^{-1}]	4936.6	145.7	49.5	3003.0
$< I_e >$	[mA]	18.7	18.0	17.9	17.1
$< I_p >$	[mA]	55.9	57.4	49.8	41.0
$< L >$	[μb^{-1}s^{-1}]	2.245	1.455	1.145	1.290
$< L_{sp} >$	[μb^{-1}s^{-1}mA^{-2}]	0.408	0.270	0.240	0.334
Bunches	$(ep + e + p)$	174 + 15 + 6			153+15+17
$< HV_{corr} >^{\dagger}$	[%]	9.1	7.9	46.2	2.1

Some more properties of the 1995 data are shown in Fig.2. One can see for example, that $\sim$ 60% of all physics data are taken in phase 2. Another "feature" of the H1 operation in 1995 is illustrated by the bottom part of this figure: the majority of the physics triggers were down-scaled. Hence the actual collected luminosity per subtrigger is visibly smaller than the total $\mathcal{L}_{G+M}$ (dashed line in the figure).

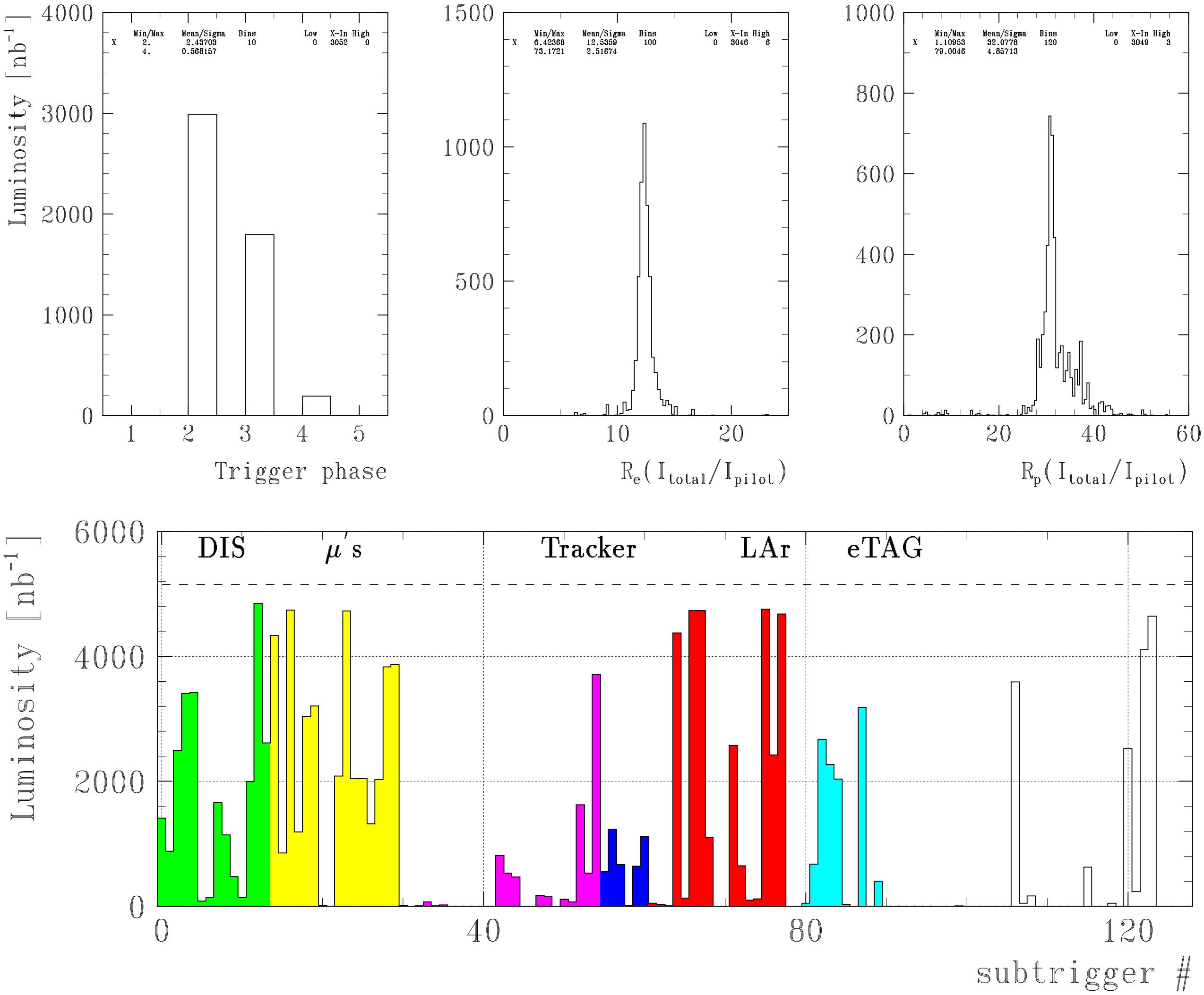

Figure 2: Some general characteristics of e$^+$p collisions in physics runs of 1995.

3 Offline Luminosity Determination

An integrated luminosity has been determined for three basic data samples, introduced in previous section (see table 3). They were further subdivided into a smaller sub-samples, if a significant change was observed in any of the critical parameters, such as a horizontal offset of the beam trajectory in the IP w.r.t. H1 axis (as measured by the CJC), the online luminosity system set up (high voltage settings, timing), accidents with the positron beam losses, which could influence the behavior of the lumi detectors and the background conditions, etc. In total 19 different run periods have been defined and analyzed.

In order to achieve high precision in the determination of $\mathcal{L}$ through eq.(3) one has to understand in great details:

- the measured E_γ spectrum, especially an absolute energy scale around E_{min},
- the background from e^+gas bremsstrahlung,
- **s91** trigger efficiency ϵ_{trig},
- geometrical acceptance of the photon arm A_γ,
- a pile-up effect.

3.1 General Properties. Choice of E_{min}

The energy distributions at different luminosity detectors are shown in Fig.3. A large tail at $E_\gamma > 30$ GeV is due to pile-up effect. The energy resolution of the crystal calorimeters ET and PD corresponds to $\sim 15\%/\sqrt{E}$, with E in GeV. It is the same, as in a second half of the 1994 running period and worse, compared to 1992–93 conditions, where it was found to be $\sim 10\%/\sqrt{E}$.

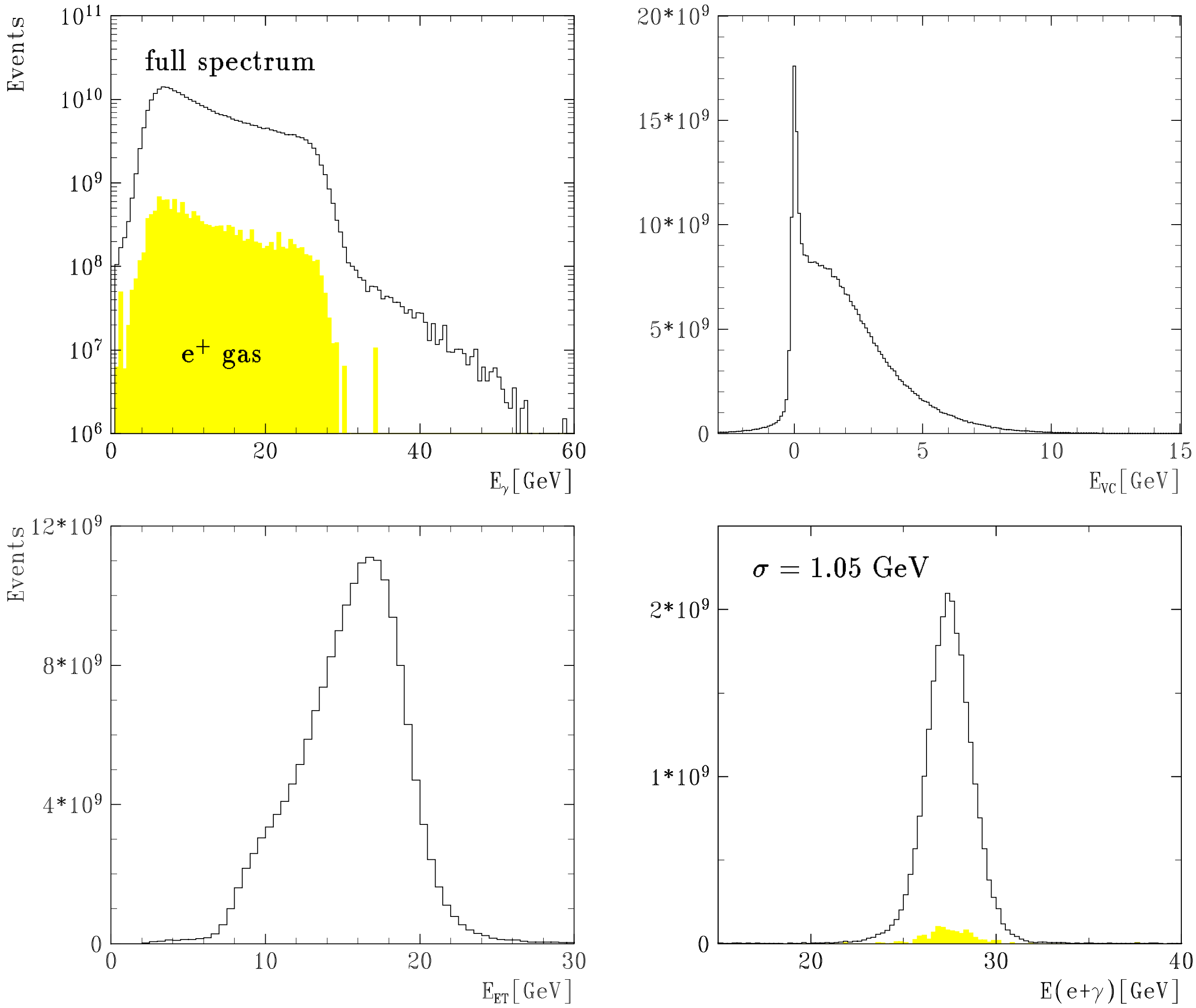

Figure 3: The energy spectra at different Luminosity detectors for BH events triggered by the **s91** condition. Shaded histograms represent a background contribution.

As it was mentioned in Introduction, the choice of E_{min} cutoff is dictated by the requirement of minimizing an overall systematic error $\delta\mathcal{L}$. Very qualitatively (quantitative arguments will be given later in this section, while describing each topic one by one in details):

- low E_{min} leads to a smaller pile-up effect corrections, but to larger uncertainties in σ_{BH} (due to various coherent effects [8, 9]) and in the trigger efficiency;
- high E_{min} increases a precision of the absolute photon energy scale (being closer to the sensitive area around E_{e-beam}, used in the fit procedure, described below), but needs large pile-up corrections.

As a result, $\boxed{E_{min} = 10 \text{ GeV}}$ was found to be an optimal value, while $E_{min} = 5$ GeV and $E_{min} = 20$ GeV were used for cross check, since they lead to partially different systematic errors.

3.2 e^+gas background

The background to reaction (1) is shown in Fig.3 as shaded histograms. It was determined from the e^+ pilot bunch events re-weighted with an additional factor $R_e = I_e^{total}/I_e^{pilot}$, and statistically subtracted from full distributions. The fraction of the background events reflects the vacuum quality in the beam pipe around the IP. A long term history of the background conditions is shown in Fig.4. For the purpose of this plot the data taken in May'95 were used as well.

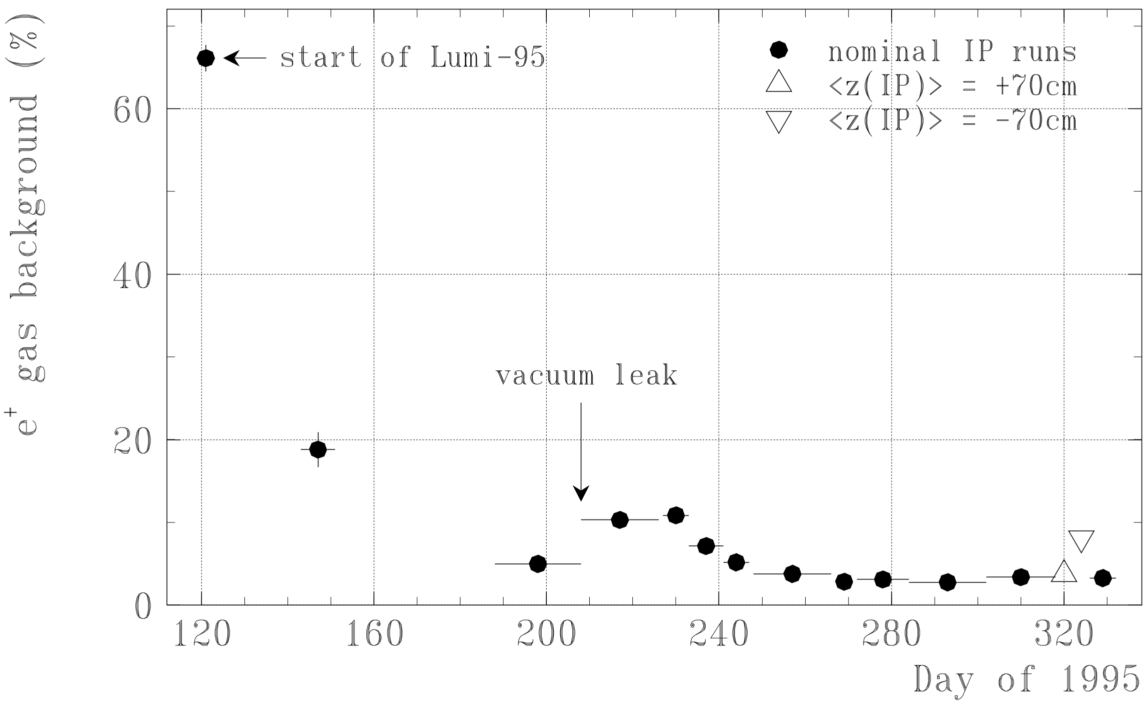

Figure 4: A long term history of the fraction of BH events, originating from e$^+$gas bremsstrahlung.

One can see, that – as expected – the vacuum was improving significantly with time. Two exceptions in this plot are related to the accident with the vacuum leak (29–July) and to hard background conditions during the exercise with $z_{IP} = -70$ cm. A stable vacuum was achieved by the end of September'95, with a plateau level of about 2 times better compared to the corresponding 1994 conditions, where it was $\sim 6 \div 7\%$.

The average levels of the e^+gas bremsstrahlung background to reaction (1) in three analyzed samples were as low as 4.4%, 3.9% and 8.2% correspondingly, thus allowing to reach a high precision of the background subtraction.

We have also checked an interesting suggestion [10] to look for a signal, originating from the positron annihilation on the electrons of rest gas:

$$e^+e^- \to \gamma\gamma.$$

Such a process should lead to a visible "peak" in E_γ distribution around E_{e-beam} energy. It can be potentially used as an additional possibility for the energy calibration of the Photon arm. No significant deviation has been observed from the expected e^+gas bremsstrahlung energy distribution, as illustrated by Fig.5. The comparison with e^-gas spectrum (from 1994 e^-p runs) leads to the same conclusion. Most obvious explanation of the absence of the expected e^+e^- annihilation contribution is, that the residual gas in the beam pipe is highly ionized.

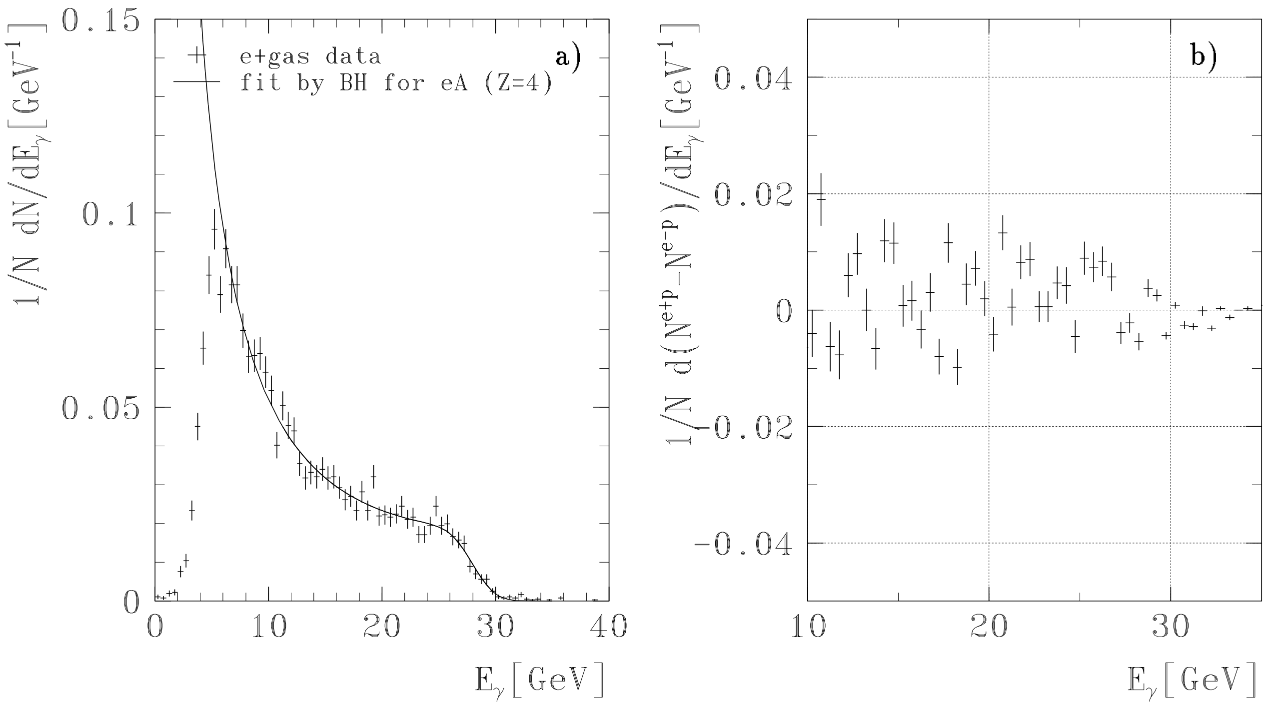

Figure 5: a) Photon energy distribution in e^+ pilot bunch events, compared to BH cross section expectation for eA bremsstrahlung on $\overline{Z} = 4$ gas, taking into account $\gamma-$arm energy resolution; b) The difference between the normalized photon energy spectra, derived from the pilot bunch events of years 1995 (e^+gas) and 1994 (e^-gas).

3.3 Trigger efficiency

The efficiencies of the trigger elements of the H1 Luminosity system are shown in Fig.6. The photon arm trigger bits efficiencies have been determined from the random trigger sample, while for the electron arm elements the **s91** events were used.

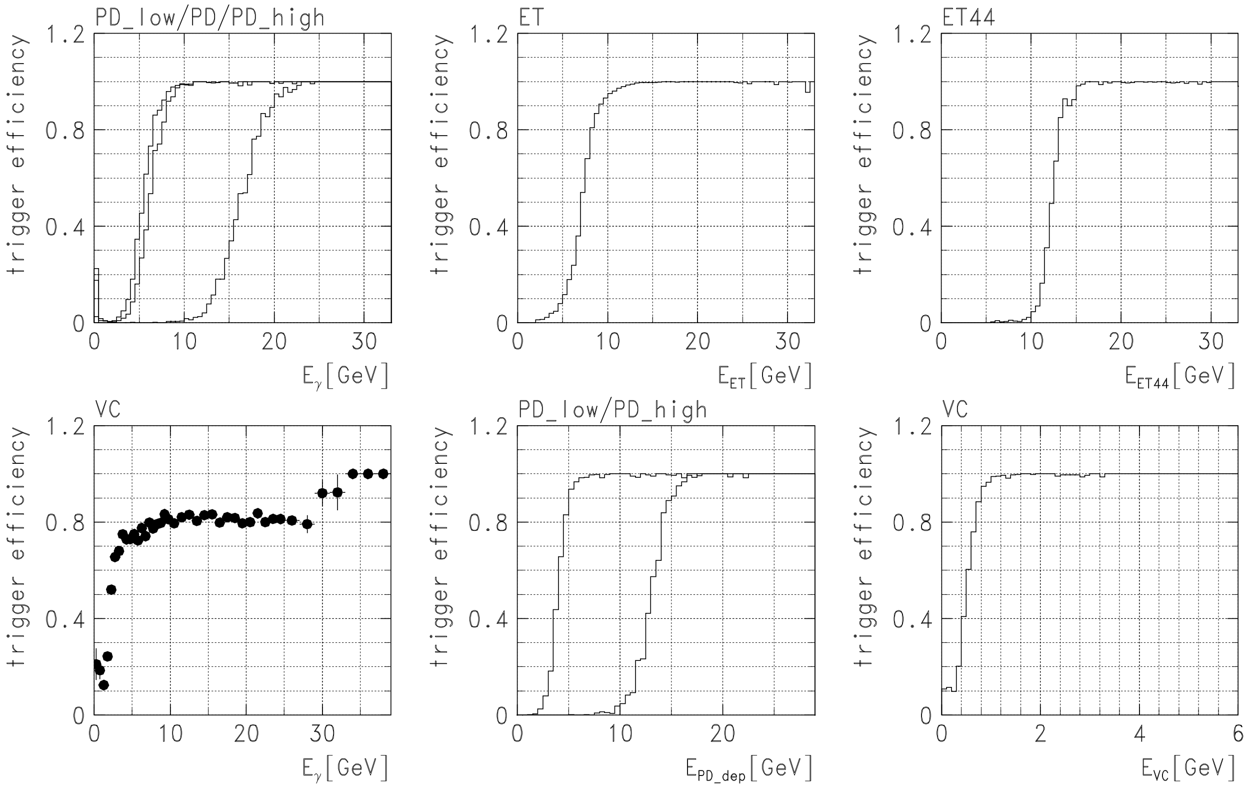

Figure 6: The trigger efficiencies of the different Lumi trigger elements in 1995.

One fact to notice is the "sharpness" of the PD-bits trigger thresholds, which are visibly better as a function of the deposited energy in the PD, compared to the total photon energy E_γ. The main reason is the influence of the Veto detector energy E_{VC}, having large fluctuations. Another interesting point is the shape of the VC-bit efficiency curve as a function of the total photon energy. The plateau level is changing from $\sim$0.8[1] to $\sim$1.0 at high E_γ, reflecting a pile-up effect (multiple photons in the same event). Note also, that this plot represents in fact a convolution of the VC efficiency with the probability of the photon to convert within $3X_0$ material.

Most relevant for present analysis is the efficiency of the subtrigger **s91** (`PD_low` bit):

$$\boxed{\epsilon_{s91}(E_\gamma > 10\ \mathrm{GeV}) = 0.9977 \pm 0.0008}$$

[1]This is somewhat less than in 1992–94, as a consequence of the modifications made in 1995 [11]. Namely, the effective thickness of the "dead" material in the photon arm was increased from $2.0X_0$ to $2.22X_0$ by adding another small water counter for the purpose of permanent beam monitoring. At the same time a depth of the "active" Čerenkov VC was reduced from $1X_0$ to $0.78X_0$.

3.4 Acceptance of the Photon Detector

The geometrical acceptance of the Photon detector for BH events is one of the most significant sources of systematic error to the luminosity measurement. It is mainly determined by the e-beam parameters, such as the horizontal and the vertical tilts θ_x, θ_y and the beam emittance, defining the angular divergence of the beam leptons, and hence the irradiated photons. The angular acceptance of the photon arm of the H1 Luminosity system is ~ 0.45 mrad, which is large compared to the typical "physics" angles of BH photons (~ 0.02 mrad). The angular divergences have to a good precision the Gaussian shapes with the widths (at the nominal e-beam optics [12]) $\sigma(\theta_x) \simeq 0.13$ mrad and $\sigma(\theta_y) \simeq 0.045$ mrad.

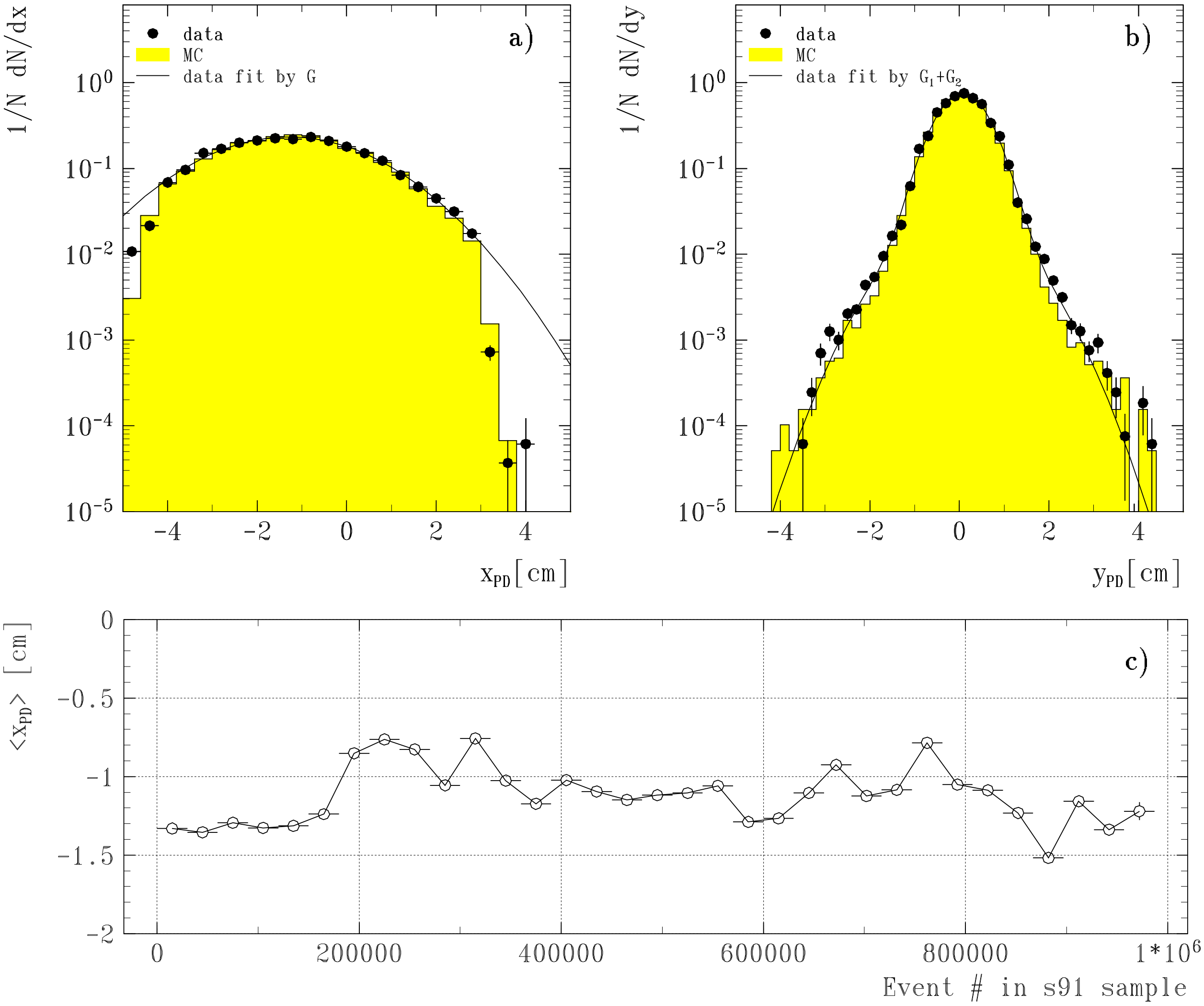

Figure 7: The photon coordinate distributions at PD (a,b) and a long term history of the horizontal e^+ beam tilt $\theta_x = < x_{PD} > /(z_{IP} - z_{PD})$ (c).

The beam tilt and divergence can be monitored experimentally by the coordinate distributions of photons at the Photon detector, as shown in Fig.7. The data are compared to Monte Carlo simulation [13], which takes into account real beam optics and the aperture limitations by the HERA magnet elements (clearly visible at the x-coordinate distribution tails).

The acceptance losses have been determined from the Monte Carlo using the lepton beam parameters, tuned to describe the measured coordinate distributions, and from the data themselves, by fitting the regions, not affected by the aperture cuts. The main systematic error in this procedure is related to the short term variations of the beam tilt, caused by slight instabilities of the HERA magnets in the H1 IP region (not visible in Fig.7c). Another source contributing to the systematic error is a possible deviation of the beam angular divergence distributions from the Gaussian shape (seen for example in the y-coordinate distribution). The final value, used for the integrated luminosity determination, is

$$\boxed{< A_\gamma >= 0.972 \pm 0.006}$$

This is somewhat worse compared to year 1994, when a narrower x_{PD}-distribution has been observed.

3.5 Photon Energy Scale

The determination of the absolute energy scale around E_{min} cutoff is one of the most crucial problems in a whole offline luminosity business.

After an overall calibration of the system (using the constraint $E_e + E_\gamma = E_{e-beam}$), the photon energy scale is verified (and if necessary – corrected), by fitting the high energy part of the E_γ spectrum between (12$\pm$2) and (30$\pm$1) GeV by BH formula [1] convoluted with the detector resolution function. The systematics of this method – including energy scale shift due to a pile-up effect – has been studied with Monte Carlo simulated events. It was found, that for a typical 1995 sub-sample ($40 \div 100K$ events) the precision of the energy scale determination (at $E_\gamma \approx 25 \div 30$ GeV) is $\sim 0.25\%$. For the complete nominal IP sample,

$$\boxed{\delta E_{\gamma-scale}(27.5 \text{ GeV}) = 0.15\%}$$

To determine the absolute scale at smaller energies is more problematic. The linearity of the Photon detector itself has been studied at test beams in 1990–91, and was found to be better than 0.4%. However, the linearity of the whole photon arm, including the Veto detector response, should be extracted from real data. One possibility is to exploit the energy correlation between the photon and the electron arms, as shown in Fig.8. Plotting the average value of $< E_e + E_\gamma >$ versus the photon energy, one can in principle extract the information on the absolute scale at lower E_γ. Naively, any deviation from the constant level line in such a dependence would mean a nonlinearity of the energy scale. Unfortunately, this simple picture is deteriorated by the limitations in the detector acceptances, especially the ET acceptance, which is strongly energy dependent. Therefore, it is necessary to compare the data with Monte Carlo events, having an ideal energy scale. Such a comparison is presented in Fig.8(b,c). For these plots the multiple photon events have been suppressed by the requirement $E_{VC} < 0.5$ GeV. One can see, that the general trends are well reproduced by Monte Carlo [13]. The residual differences, in the region of non-negligible ET acceptance, do not exceed 0.7% level. They can be treated as a consequence of the non ideal Electron

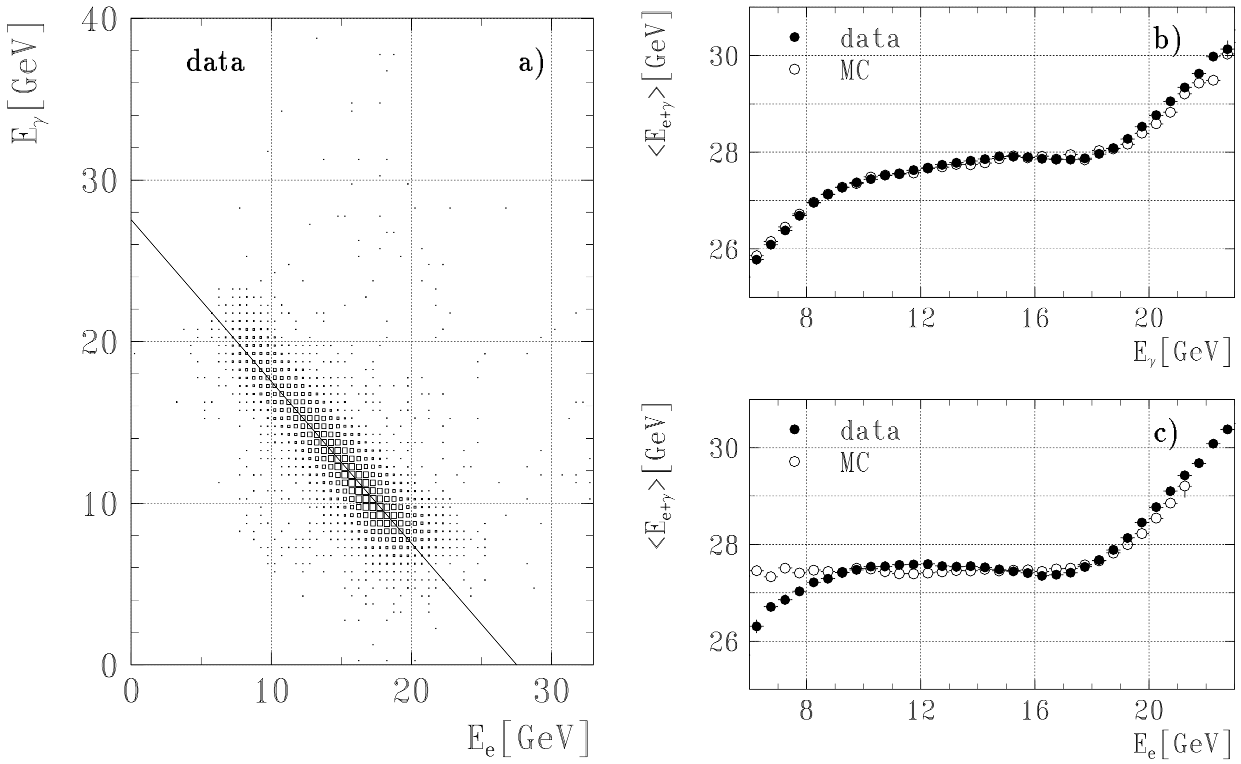

Figure 8: Energy correlations between the electron and the photon arms for BH events triggered by the coincidence requirement `ET && PD`.

tagger acceptance description in Monte Carlo. From that we conclude, that the data are compatible with a simple scale error propagation:

$$\delta E_\gamma(E_{min}) = \delta E_\gamma(E_0)\frac{E_0}{E_{min}}.$$

The final step is to translate δE_γ to $\delta \mathcal{L}$ through the non-linear dependence $\delta\sigma_{BH}(\delta E_{min})$. As an example, the following systematic errors are obtained for the nominal IP data sample:

$$\delta\sigma_{BH} = \begin{cases} 0.74 \cdot \delta E_\gamma = 0.61\% & for\ E_{min} = \ 5\ GeV, \\ 1.13 \cdot \delta E_\gamma = 0.47\% & for\ E_{min} = 10\ GeV, \\ 2.98 \cdot \delta E_\gamma = 0.62\% & for\ E_{min} = 20\ GeV. \end{cases}$$

3.6 Pile-up Effect

The photon pile-up – i.e. more than one BH photon at the same bunch crossing within the acceptance of the H1 Luminosity System – cannot be neglected at HERA. A probability of the multiple photons overlap is described by a Poisson distribution with mean value μ related to luminosity L as

$$\mu = \frac{\sigma_{BH}(E_\gamma > \epsilon) \cdot L}{f_{HERA} \cdot N_{ep}}, \tag{4}$$

where $\epsilon \approx 150$ MeV is a minimal energy of the photons, which can still penetrate a filter in front of VC and PD and deposit some visible energy to their response. N_{ep} is a number of colliding bunch pairs, and $f_{HERA} = 47.35$ kHz is a revolution frequency of the HERA machine. For $\mu \ll 1$, which is valid for all 1995 conditions ($N_{ep} = 174$), this leads to a simple relation

$$\boxed{P(n\gamma) = 1 - e^{-\mu} \approx (3.2 \pm 0.2)\% \cdot L} \tag{5}$$

with L in $\mu b^{-1}s^{-1}$. Main uncertainties come from the large corrections to BH formula at such small energies [8, 9], and from the precision of the ϵ estimate (made using a detailed MC simulation of the Photon arm response to low energy photons).

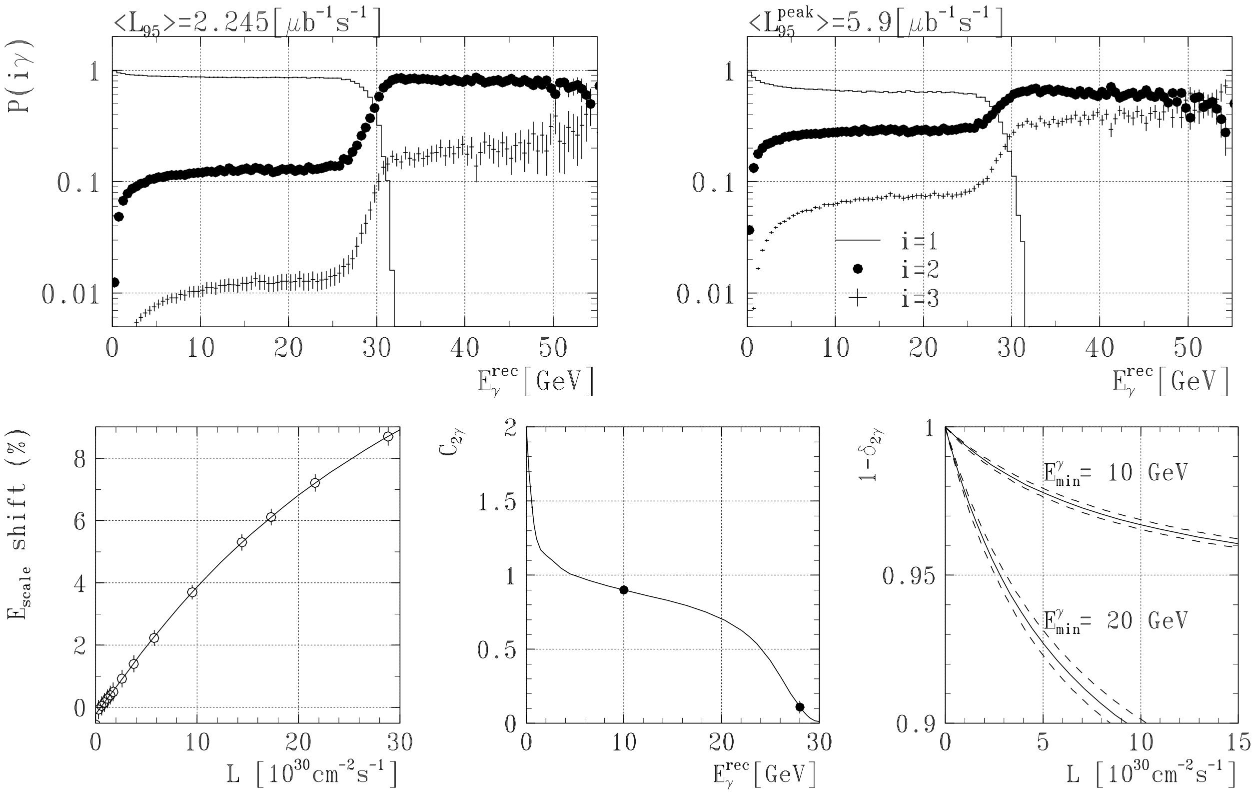

Figure 9: MC simulation of the photon pile-up effect. Top: relative fractions of the events with different photon multiplicities. Bottom: correction factors used for the offline $\mathcal{L}_{1995}$ determination. Symbols and dashed curves represent the systematic errors of the corresponding factors.

The photon pile-up leads to the following effects, which have to be corrected for:

1. luminosity dependent shift of the energy scale in the fitting procedure of the E_γ spectrum and
2. the difference between visible and predicted by σ_{BH} number of photons with $E_\gamma > E_{min}$. The latter in turn can be further split into two parts:
   - the migration correction in $n\gamma$ events $C_{n\gamma}(E) = N_{BH}^{true}(E_\gamma > E)/N_{BH}^{obs}(E_\gamma > E)$,

- a fraction of the $n\gamma$ events in the studied sample, which also depends on the value of E_{min}.

Thus, the final $\delta_{n\gamma}$ correction factor in (3) depends both on L and E_{min}.

Note, that in practice we only accounted for up to 3γ overlaps, neglecting 4 and more photon events, as their probability is very small at present HERA luminosities.

The pile-up effect has been studied using large statistics H1LUMI MC simulation [13] with the real energy resolution derived from the data. The results are summarized in Fig.9. One can see, that $E_{min} = 5$ GeV is the best value for minimizing the pile-up corrections. In fact, at this value the migrations are fully compensated[2]. The luminosity dependence of the 2γ overlap correction factor for the two other values of E_{min} is shown in the last plot of Fig.9. The dashed curves correspond to the systematic error band.

Fig. 10 shows the photon energy distributions in three data samples of 1995, compared to Monte Carlo expectations taking into account 2γ and 3γ overlap events. The agreement between the data and Monte Carlo at $E_\gamma \geq 10$ GeV is quite good. The fall off at smaller energies is due to the trigger threshold, not simulated for this study.

3.7 Corrections to the Online Luminosity

The final result, obtained with $E_{min} = 10$ GeV, is presented in Fig.11 as a correction to the online luminosity measurements for 19 different run ranges of 1995. The correction is defined as $\Delta\mathcal{L} = (\mathcal{L}_{offline} - \mathcal{L}_{online})/\mathcal{L}_{online}$. There is no clear explanation for a large correction value in the first run period, except that there was a LUMI FADC timing adjustment made, after the Central Trigger hardware upgrade. In any case, this subsample contains only ~ 9 nb^{-1} of data representing less than 0.2% of the statistics analyzed.

One can see, that there is an obvious correlation between the size of the luminosity correction and the horizontal offset of the reference e beam trajectory in the H1 IP region, as measured by the CJC [14]. It is known, that the ET acceptance is very sensitive to both the beam tilt and the position of the trajectory in the horizontal direction. Thus, the result shown in Fig.11 confirms the hypothesis that the Electron tagger acceptance variation is the main reason for the systematic error in the absolute luminosity determination by a coincidence method.

In average, the corrections to the online luminosity for three main data samples are:

Data sample	Nominal IP	$< z(IP) >= +70$cm	$< z(IP) >= -70$cm
$\Delta\mathcal{L}$	-2.7%	-5.4%	-1.2%

A cross check has been performed for the nominal IP sample by using $E_{min} = 5$ GeV and $E_{min} = 20$ GeV. The result, presented in table 4, shows no apparent problems in the analysis. Note, that the common part of the systematic error is excluded from the table and from the comparison of the three $\mathcal{L}$ values obtained.

[2] I.e. $N_{+1}(E_{\gamma 1} < E_{min};\ E_{\gamma 2} < E_{min};\ E_{\gamma 1} + E_{\gamma 2} > E_{min}) = N_{-1}(E_{\gamma 1} > E_{min};\ E_{\gamma 2} > E_{min})$.

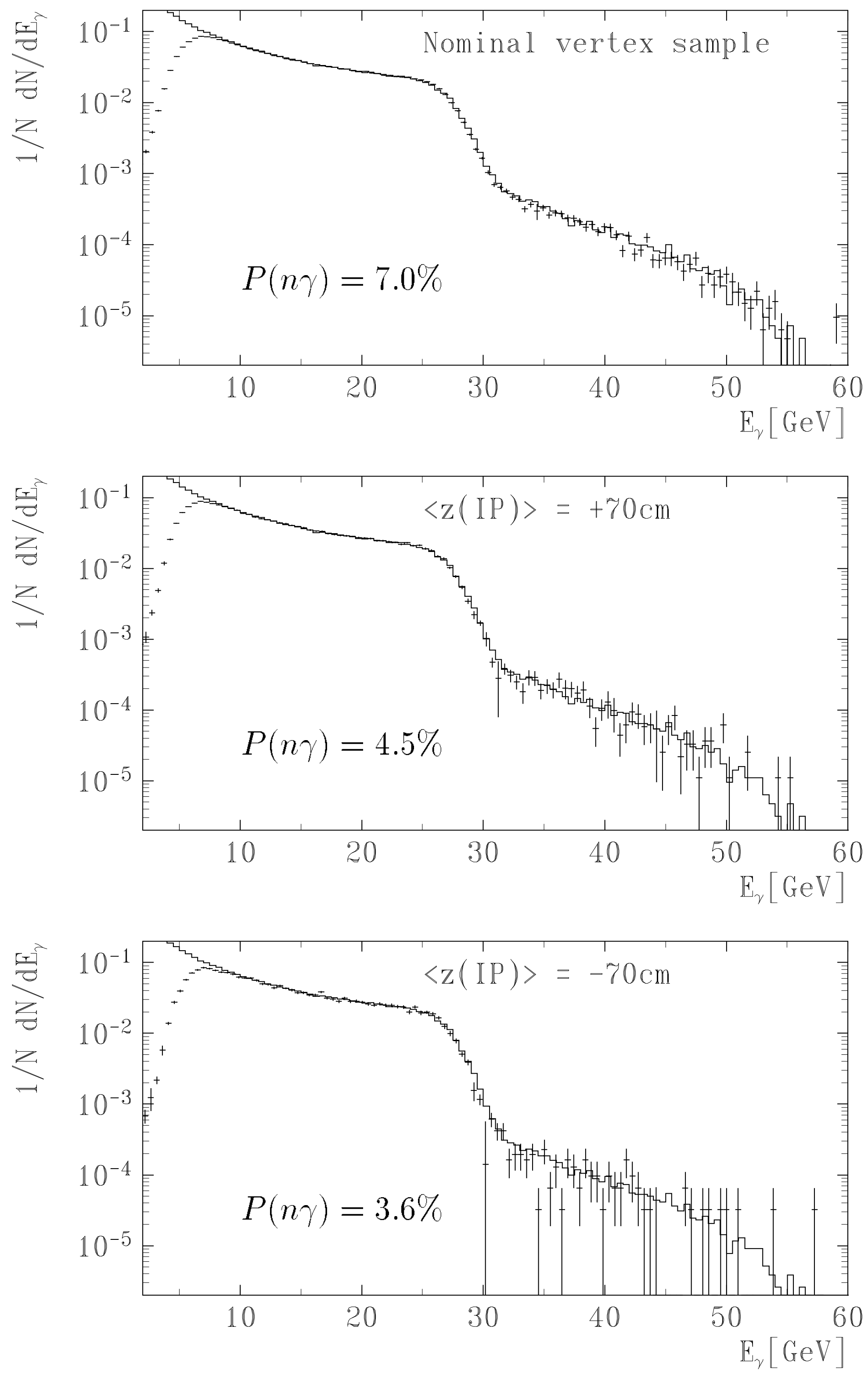

Figure 10: The photon energy spectra (symbols) in three different data samples of 1995, compared to Monte Carlo expectations (histograms) taking into account the detector resolution and a multiple photon overlap effects. The probabilities $P(n\gamma)$ used in MC were calculated using eq.(4–5) and actual luminosities, averaged over all G and M runs in a given sample.

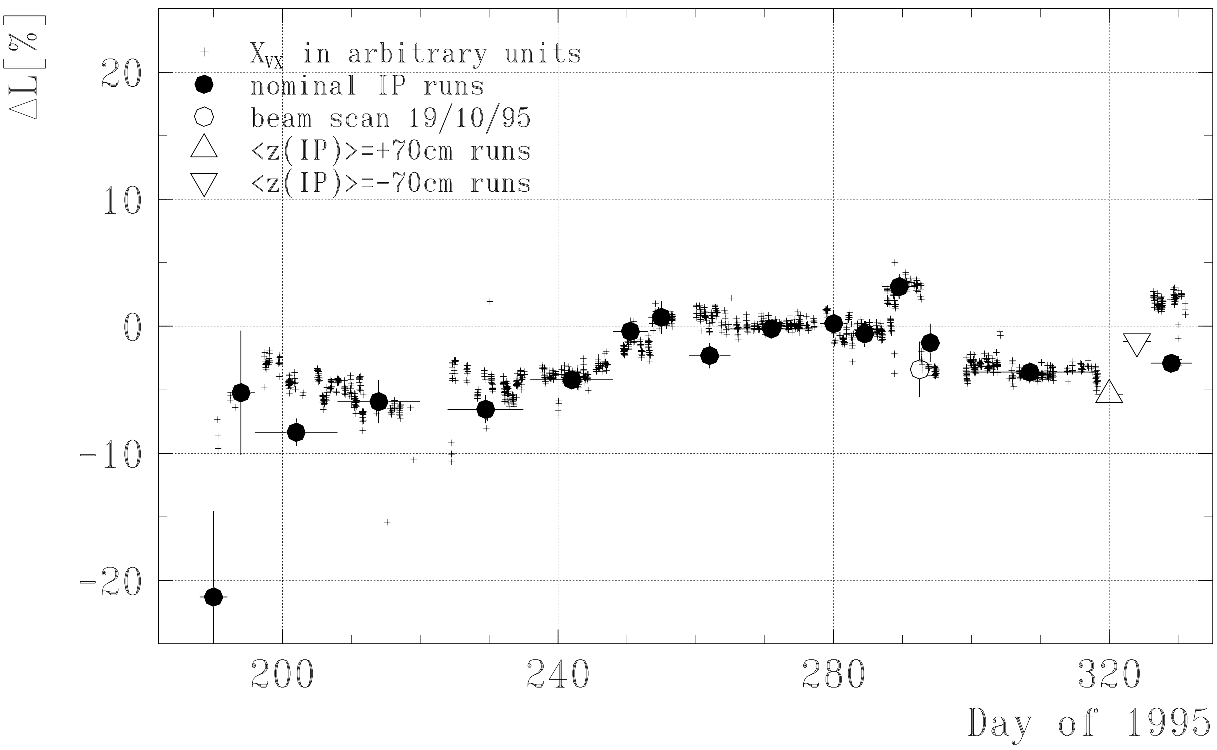

Figure 11: Offline correction to the 1995 online luminosity measurements. Overlayed (as small crosses) are the horizontal positions of the e^+p event vertecies (in arbitrary units) as measured by the CJC and averaged over the long H1 runs.

Table 4: Comparison of the integrated luminosity values for the nominal IP sample, obtained by using different E_{min} cutoffs. The common part of the systematic error is excluded from the table. σ_{BH}^{acc} is the acceptance corrected BH cross section.

Value	Unit	$E_{min} = 5$ GeV	$E_{min} = 10$ GeV	$E_{min} = 20$ GeV
$\sum W_{ep}$	$[10^9]$	298.41 ± 0.48	180.46 ± 0.38	54.28 ± 0.20
ϵ_{trig}		0.9035 ± 0.0031	0.9977 ± 0.0008	0.9989 ± 0.0006
$\delta_{n\gamma}$		0.0	0.0123 ± 0.0011	0.0425 ± 0.0036
σ_{BH}^{acc}	[mb]	69.31 ± 0.50	37.28 ± 0.18	10.83 ± 0.07
$\mathcal{L}$	$[\mathrm{nb}^{-1}]$	4765 ± 38	4792 ± 24	4805 ± 38
$R = \frac{\mathcal{L}(E_{min})}{\mathcal{L}(10GeV)}$		0.9944 ± 0.0094	1.0	1.0027 ± 0.0094

3.8 Systematic Error Summary

All specific contributions to the overall systematic error $\delta\mathcal{L}$ are collected in table 5. For comparison, the precisions of the integrated luminosity determination in previous years are included as well. Some of the systematic error contributions for 1994 data were re-evaluated in order to be consistent with the present analysis (i.e. to have the same meaning). It is very hard to improve further a precision of the luminosity measurement by this method.

The "Rounding errors" row refers to a precision of calculating the integrated run luminosity, including corrections for the detector HV status. Note, that this is not directly related to the luminosity system performance. In addition, it is in general analysis dependent, because different analyses require different H1 configurations. Presently there is no good model to calculate the precision of the HV correction accurately. All realistic estimates based on simple statistical considerations lead (for H1 configuration as in table 3) to the values safely below 0.1%. The rounding errors related to the 10 sec online measurement sampling are in average of same order: $\delta\mathcal{L}_{RUN} \leq 10\% \cdot (10sec/t_{RUN}) \approx 0.1\%$. Therefore, the corresponding values in table 5 should be considered as a temporary additional safety margins.

Another room for possible improvement is related to the theoretical precision of the BH formula, used for normalization. A numerical evaluation of higher order corrections and various coherent effects is necessary to reach an ultimate precision in that area.

Table 5: Precision (in %) of the H1 integrated luminosity determination in 1995, compared to 1993 and 1994 data (satellite bunch corrections are not included here).

Contribution to $\delta\mathcal{L}$	1993	1994			1995		
		e^-p	e^+p	sh.IP	nominal	+70cm	−70cm
1. Theoretical value for σ_{BH}	0.5		0.5			0.5	
2. Trigger efficiency	2.0		0.3			0.1	
3. Statistics, e-gas bgr. subtraction	1.5	1.3	0.4	3.3	0.21	0.41	0.77
4. γ-energy scale (calib. & resol.)	1.7	1.2	1.0	1.7	0.47	0.50	0.79
5. Geometrical acceptance of γ-arm	0.7		0.5			0.6	
6. Multiple photon effect (pile-up)	0.2		0.1		0.11	0.09	0.06
7. Rounding errors (HV corr. etc.)	1.1		0.5			0.5	
Total error from the lumi system	3.4	2.0	1.4	3.8	1.07	1.14	1.45

4 Satellite bunch correction

The last and significant correction to the integrated luminosity for physics analysis is related to the presence of the parasitic satellite bunches in the proton beam of HERA. These satellites give rise to ep events outside the $z-$vertex acceptance cutoff.

The procedure used in the present analysis is fully analogous to those described in [15]. FToF spectra were extracted from `BRTQ` banks, collected only during G and M runs. This reduces a statistical significance, but improves the systematics, since it was observed, that the satellites are usually decaying faster, than the main proton bunches. As a consequence, their relative contribution to G and M runs (collected mostly towards the end of Lumi fills) are smaller than the average over the full luminosity run.

Approximately 92% of all luminosity runs contain statistically significant FToF information. The determination of the satellite structure was made for each of those ep collision

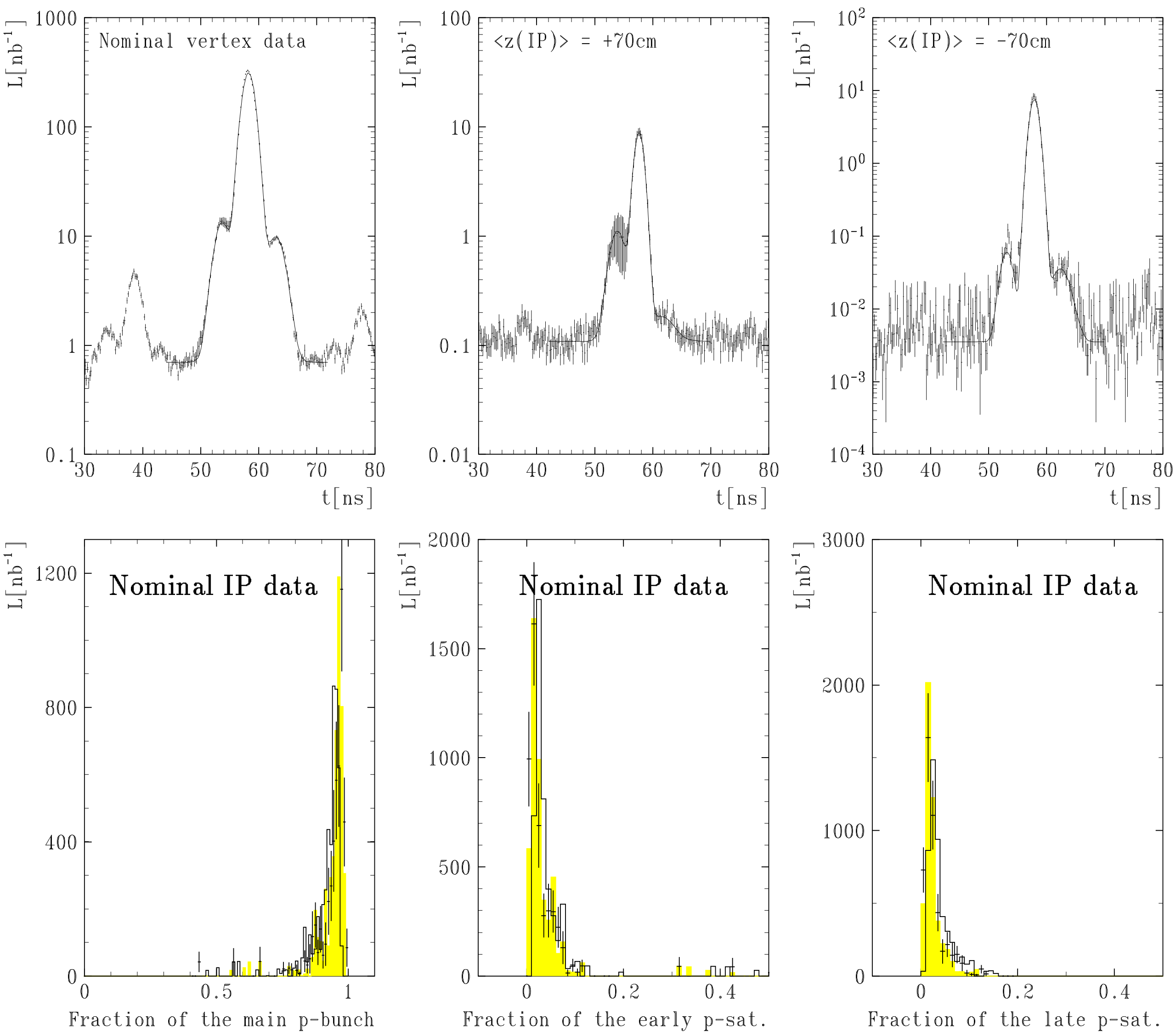

Figure 12: Top: FToF spectra accumulated in "G" and "M" runs of 1995 e^+p collisions. The curves represent the results of the fit by (6). Bottom: luminosity weighted fractions of the main proton bunch together with closest ± 4.8 ns p-satellites in the nominal IP sample, estimated by three different methods explained in the text.

runs, and for the luminosity weighted average spectra for the three main data samples of 1995. The latter are shown in Fig.12.

FToF spectra were fitted in [42ns, 72ns] time intervals by a superposition of three Gaussians and a constant background:

$$F(t) = G(A_0, t_0, \sigma_0) + G(A_1, t_1, \sigma_1) + G(A_2, t_2, \sigma_2) + P_0. \tag{6}$$

In average, the distances of 4.61 ± 0.02 ns (4.75 ± 0.03 ns) were found between the main proton peak and early (late) satellites. This is very close to a "theoretically" expected 4.8 ns. So called "20 ns satellites" (or more precisely 19.2 ns) are also seen in the figure. They were included in the "tails" of the proton bunch distributions.

Relative fractions of the closest to the main proton peak early ("forward" in H1 coordinate system) and late ("backward" in H1) satellites were determined using the following estimators:

- the amplitudes A_i of the corresponding Gaussians,
- the full areas under the Gaussians, S_{G_i},
- the sum of the weights in FToF histograms within $\pm 2.5\sigma$ around mean values t_i.

The spread of the results, shown in the bottom part of Fig.12, gives an estimate of the systematic uncertainty. As a central values the S_{G_i} estimators were used, obtained from the combined luminosity weighted FToF spectra (Fig.12). The tails were estimated by counting the total number of entries below 48 ns and above 68 ns.

The results are summarized in table 6. The row labelled "$\mathcal{L}$ used" shows which fractions of the data samples had an FToF information available.

Table 6: A relative intensity of the different parts of the FToF spectra, reflecting a complicated time structure of the proton bunches in 1995 data samples, and an estimate of the satellite bunch corrections to physics luminosity.

Part of the FToF spectra	Fraction (%)		
	nominal IP	$< z(IP) >= +70$cm	$< z(IP) >= -70$cm
I(main peak)	91.4 ± 0.8	89.9 ± 1.3	99.6 ± 0.1
I(-4.8ns sat)	4.2 ± 0.5	8.4 ± 1.2	0.3 ± 0.1
I($+4.8$ns sat)	3.0 ± 0.6	0.8 ± 0.4	0.1 ± 0.1
I(tails)	1.4 ± 0.2	0.9 ± 0.3	–
$\mathcal{L}$ used	91%	93%	98%
$\Delta\mathcal{L}_{sat}$ (%)	$3.6 \pm 0.4^{+1.6}_{-0.3}$	$4.6 \pm 0.7^{+2.1}_{-0.4}$	$0.2 \pm 0.1^{+0.09}_{-0.02}$

In order to determine a fraction of the integrated luminosity, originating from the satellites and more distant tails of p-bunches (and excluded from the standard physics analyses), the first method was used, as described in [15]. Namely:

$$\mathcal{L}_{sat} = \mathcal{L}_{sp}(z_{sat}) \cdot \sum (I_e I_p^{sat}), \tag{7}$$

where the sum is taken over all pairs of colliding bunches. This led to an additional systematic error related to the assumption, that it is p-wall background which mainly contributes to FToF spectra, rather than p-gas (see eq.(3,4) in [15]). Such an assumption (based on the 1994 results) can only be verified by analyzing the least biased $z-$vertex distributions of physics events in 1995 data, e.g. low Q^2 DIS sample (not available for present analysis), or by a direct measurement of the proton current time structure with a fast pick-up device (foreseen for 1996 data).

The values of the satellite bunch correction to the integrated luminosity are given in the last row of table 6. The first error is related to the precision of the FToF spectra analysis, and reflects also the size of the possible final error after exploiting a $z-$vertex method [15]. The second asymmetric error originates from the limitations of the method based on (7), and should be added until the $z-$vertex analysis is performed.

5 Conclusions

It has been shown, that three types of correction to the online luminosity measurement have to be applied for 1995 data samples:

1. $\Delta\mathcal{L}_{off}$ – due to electron tagger acceptance variations,

2. $\Delta\mathcal{L}_{HV}$ – for the detector high voltage status and

3. $\Delta\mathcal{L}_{sat}$ – due to the proton satellite bunches effect.

The last two are not related to the H1 luminosity system performance.

The database has been updated with a new set of `LOFF` banks, such that a standard H1 lumi tools [16] return the luminosity values corrected for the first two effects. The satellite bunch corrections should be applied additionally, and so far "by hand", until the final $z-$vertex analysis is performed.

High precision is achieved in the integrated luminosity determination of 1995 data samples. It is presently limited by the knowledge on the proton satellite bunch correction.

These results are summarized in a final table 7, where the values for HV correction refer to the following fully operational detector configuration: CJC, LAr, Spacal, ToF, Lumi.

Table 7: Average corrections ($\Delta\mathcal{L}, \%$) to the online luminosity measurement for 1995 data samples, and precision ($\delta\mathcal{L}, \%$) of the integrated luminosity determination.

Data sample	nominal IP	$< z(IP) >= +70$cm	$< z(IP) >= -70$cm
$\Delta\mathcal{L}_{off}$	-2.7	-5.4	-1.2
$\Delta\mathcal{L}_{HV}$	-9.1	-7.9	-46.2
$\Delta\mathcal{L}_{sat}$	-3.6	-4.6	-0.2
$\delta\mathcal{L}_{lumi}$	1.07	1.14	1.45
$\delta\mathcal{L}_{sat}$	$0.4^{+1.6}_{-0.3}$	$0.7^{+2.1}_{-0.4}$	$0.1^{+0.09}_{-0.02}$

Acknowledgements

We would like to thank A.Fomenko for supporting this analysis with the energy calibration of the Luminosity detectors for all 1995 data samples.

Appendix

FPACK classification. A special event classification is implemented, which is only valid for `LUMIMON` data, to provide an easier access to different classes of luminosity monitoring events in the analysis.

```
+=====================================================================+
|          FPACK  classification  scheme  (Class = bit+1)             |
|---------------------------------------------------------------------|
|       |      |            |                         |               |
| Bunch | Trig |    LREC    |        Sub_Trig         |    Trig_El    |
|  e p  | Set  |  Section   |        section          |    section    |
|       |      |            |                         |               |
|---------------------------------------------------------------------|
|  2 2     2     2 2 2 2 2   1 1 1 1 1 1 1 1 1 9 8   7 6 5 4 3 2 1 0 |
|  7 6     5     4 3 2 1 0   9 8 7 6 5 4 3 2 1 0                     |
+=====================================================================+
```

```
 F-class      Content
 ---------------------------------------------------------------------
    1         LUMI trigger bit 0 is set (LU_PD_high)
    2         LUMI trigger bit 1 is set (LU_PD_low)
    3         LUMI trigger bit 2 is set (LU_ET_44)
    4         LUMI trigger bit 3 is set (LU_ET)
    5         LUMI trigger bit 4 is set (LU_PD)
    6         LUMI trigger bit 5 is set (LU_Wat_Vet)
    7         LUMI trigger bit 6 is set (eTAG = LU_ET && !LU_PD_low)
    8         LUMI trigger bit 7 is set (not used presently!)
 ---------------------------------------------------------------------
    9         Random trigger event
   10         Actual subtrigger s0  (SPCLe_IET>1)                   (P)
   11         Actual subtrigger s83 (eTAG && DCRPh_TNeg && zVtx_T0)  (P)
   12         Actual subtrigger s85 (eTAG_44 && zVtx_T0)            (P)
   13
   14         Actual subtrigger s86 (eTAG)                          (M)
   15         Actual subtrigger s90 (LU_ET_44)                      (M)
   16         Actual subtrigger s91 (LU_PD_low)                     (M)
   17         Actual subtrigger s92 (LU_PD && !LU_WatVet)           (M)
   18         Actual subtrigger s93 (LU_WatVet)                     (M)
   19         Actual subtrigger s94 (LU_ET && LU_PD && !LU_WatVet)  (M)
   20         Actual subtrigger s95 (LU_ET && LU_PD && LU_WatVet)   (M)
 ---------------------------------------------------------------------
   21         Event was reconstructed by LREC (at L4)
   22         Energy deposit in ET  > ET_noise_cut
   23         Energy deposit in ET1 > ET1_noise_cut
   24         Energy deposit in PD  > PD_noise_cut
   25         Energy deposit in VC  > VC_noise_cut
 ---------------------------------------------------------------------
   26         Trigger set 0 (standard collision data mode)
   27         Event from the filled proton bunch (I_p>I_p_min)
   28         Event from the filled lepton bunch (I_e>I_e_min)
 ---------------------------------------------------------------------

 Examples:    In all examples below a symbolic dataset name LUMIMON is assumed:
 ---------    (OPEN LUMIMON UNIT=1 FILE=...)  For more details see FPACK manual.

   1) select events from colliding bunches:
        SELECT  LUMIMON  CLASS=27 CLASS=28

   2) select e-pilot bunch events:
        SELECT  LUMIMON  NOTCLASS=27 CLASS=28

   3) select events taken in lumi conditions by random trigger,
      and having energy deposits in either ET, or ET_44:
        SELECT  LUMIMON  CLASS=26 CLASS=9 CLASS=22,23
```

References

[1] H.Bethe and W.Heitler, Proc. Roy. Soc. **A146** (1934) 83.

[2] H1 Collaboration (T. Ahmed, et al.), Experimental Study of Hard Photon Radiation Processes at HERA. Z.Phys. C66 (1995) 529-542.

[3] N.Gogitidze, H1 LUMI System Status Report. H1 Collaboration meeting, DESY, HH, 13-Oct-1994. (Lumi documents in WWW).

[4] H1 Collaboration (I. Abt, et al.), The H1 Detector at HERA, DESY preprint 93-103 (1993), to be published in Nucl. Instr. and Methods.

[5] V.Blobel, P.Binko, Z.Szkutnik, FPACK Manual (1993)

[6] S.Levonian, H1 Luminosity Data, `http://dice2.desy.de/h1/iww/iwork/ilumi/files.html`

[7] D.Hoffmann, F.Sefkow, H1 Trigger Information, `http://dice2.desy.de/itrigger/h1trig.html`

[8] G.L.Kotkin, S.I.Polityko, A.Schiller, V.G.Serbo, Z.Phys. **C39** (1988) 61.

[9] K.Piotrzkowski, Z.Phys. **C67** (1995) 577.

[10] A.S.Belousov, private communications (1994)

[11] A.Usik, Photon arm upgrade (1995) `http://dice2.desy.de/~usik/lumi/pharm_up.ps`

[12] G.Wolf, HERA: Physics, Machine and Experiments, DESY 86-089 (1986)

[13] S.Levonian, H1LUMI - A Fast Simulation Package for the H1 Luminosity System, H1 note H1-04/93-287 (1993)

[14] V.Blobel and L.Criegee, ONLINE monitoring and determination of run-dependent calibration constants within reconstruction modules, H1 s/w note 41 (1993)

[15] S.Levonian and A.Panitch, Treatment of the Proton Satellite Bunches in 1994 Data, H1 note H1-09/95-454 (1995)

[16] S.Levonian, H1 Luminosity tools, `http://dice2.desy.de/h1/iww/iwork/ilumi/tools.html`